Int. J. Solids Structures Vol. 16, pp 673–682
© Pergamon Press Ltd., 1980. Printed in Great Britain
0020-7683/80/0801-0673/$02.00/0

DYNAMIC EFFECTS IN THE PROPAGATION OF A DUCTILE PENNY-SHAPED CRACK

Y. M. TSAI

Department of Engineering Science and Mechanics, Iowa State University, Ames, Iowa, U.S.A.

(*Received* 17 *April* 1979; *in revised form* 3 *November* 1979)

Abstract—The propagation of an interior penny-shaped crack in a ductile material subject to uniform tension at infinity is investigated using the methods of Hankel and Laplace transforms. The crack is assumed to be the Dugdale crack which has a uniform tensile yield stress around its crack tip. Exact expressions for the finite stress condition at the crack tip, the crack shape, the crack opening displacement and the energy release rate are obtained and written as the product of explicit dimensional quantities and a non-dimensional dynamic correction function. All the expressions obtained reduce to the associated static results when the crack speed tends to zero. Using an electronic computer, the dynamic correction functions were calculated for various values of the non-dimensional parameters involved.

The size of the plastically deformed zone around the crack tip is determined from the finite stress condition. A general, convenient method is described to determine the plastic zone size using the non-dimensional dynamic correction curves. It is shown that the plastic zone width shrinks significantly with increasing crack speed. Due to the inertial effect of the material particles, the crack opening displacement and the energy release rate are also found to decrease with increasing crack speed.

INTRODUCTION

The plastic-zone size in front of a stationary slot in a metallic plate under static tension was investigated experimentally and predicted by Dugdale, using a model of ductile crack[1]. The Dugdale model predictions were found to be in close agreement with experimental results[1, 2]. The model was applied to a stationary penny-shaped crack in an infinite solid material or a finitely thick plate[3, 4].

The propagation of a Dugdale crack was investigated, using steady-state solutions[5, 6]. The finite stress conditions at the crack tip predicted that the ratio of the plastic zone size to the crack length is independent of crack speed and remains exactly the same as that for the corresponding static problems[5, 6]. However, experimental results indicate that the crack tip plastic zone in steel may shrink as the crack increases in velocity[7, 8]. The shrinkage of the crack-tip plastic zone as a function of crack speed was predicted from the finite stress condition of the Dugdale model in a recent study on the propagation of a two-dimensional central crack[9].

In elastostatic problems, the contours of equal maximum shearing stress for a two-dimensional central crack and a penny-shaped crack were presented to visualize the distribution of stress around the crack for each case[10]. In general outline, the variations of the contour curves are similar between the two cases. However, the main difference lies in their behavior near the crack edges[10].

Cracks often initiate and propagate from the interior of a solid material. To study the effect of crack speed on the behavior of a fracturing ductile material containing an interior crack, the propagation of a Dugdale penny-shaped crack is considered in the present work. Using the integral transform methods similar to those used in an earlier work[11], the shrinkage of the plastic zone and the variations of the crack shape, the crack opening displacement and the energy release rate are investigated as a function of crack speed and material properties.

STATIONARY DUCTILE CRACK

A penny-shaped Dugdale crack in an infinite solid-material is considered running in a plane perpendicular to a uniform tensile field p_0 acting on the solid. Propagation of the crack creates new stress-free crack surface with radius $l(t)$, which is surrounded by an inelastically deformed region of radius equal to $a(t)$. For a Dugdale crack, the stress in the plastic zone is prescribed as a constant tensile yield stress of material Y. Solutions of the problem can be obtained by superposing a uniform tension field p_0 and the stress field which is set up by a pressure, $-p_0$,

acting on the crack surfaces and the tensile stress $Y - p_0$, acting in the plastic annulus [3, 4]. The latter dynamic problem is the main subject of interest in the present work. To obtain solutions, cylindrical coordinates (r, φ, z) are used and the above normal stresses are described by a function at $z = 0$ as follows:

$$\sigma(r, t) = -p_0 + \begin{cases} 0, & r \le l(t) \\ Y, & l(t) < r \le a(t). \end{cases} \tag{1}$$

To solve the problem, the dynamic boundary conditions can be prescribed on the crack plane $z = 0$ for $t > 0$ as

$$\sigma_{zr} = 0 \tag{2}$$

and

$$v = \begin{cases} w(r, t), & r \le a(t) \\ 0, & r > a(t) \end{cases} \tag{3}$$

where v is the z-direction displacement normal to the crack plane and $w(r, t)$ is an unknown crack shape function to be determined in terms of $\sigma(r, t)$ in eqn (1). The methods of Hankel and Laplace transforms similar to those used in [11] can be used to solve the equations of motion and to satisfy the dynamic boundary conditions. After inversions, the normal stress on $z = 0$ can be written as obtained in [11]:

$$\sigma_{zz}(r, t) = \sigma^0_{zz} - p_0 q \tag{4}$$

where

$$\sigma^0_{zz}(r, t) = -K \int_0^\infty J_0(sr) s^2 \hat{w}^0 \, ds, \quad K = \mu/(1 - \nu) \tag{5}$$

$$p_0 q = \rho c_1 L Q_1 + \mu L_2 Q_2 \tag{6}$$

$$Q_1 = \int_0^\infty J_0(sr) s \frac{\partial}{\partial t} \int_0^t \sin [s c_1 \eta (t - \tau)] \frac{\partial}{\partial \tau} \hat{w}^0 \, d\tau \, ds \tag{7}$$

$$Q_2 = \int_0^\infty J_0(sr) s^2 \int_0^t \cos [s c_2 \eta (t - \tau)] \frac{\partial}{\partial \tau} \hat{w}^0 \, d\tau \, ds \tag{8}$$

and

$$\hat{w}^0 = \int_0^a w(r, t) r J_0(sr) \, dr \tag{9}$$

μ, ν, ρ and c_1 are, respectively, the shear modulus, Poisson's ratio, the medium density and the dilatational wave speed. $J_0(r)$ is the zeroth order Bessel function. L and L_2 are operators over η and are defined in the Appendix. In fact, L results from an integral representation of the zeroth order Bessel function [12]. L_2 results from contour integrations along branch cuts [11] and involves the quantity $k^2 = (c_1/c_2)^2 = 2(1 - \nu)/(1 - 2\nu)$, c_2 being the shear wave speed.

The integration techniques used in [3, 11] can be operated over eqn (4) to solve for the unknown $w(r, t)$. Indeed, eqn (4) is converted in terms of eqn (1) into an integral equation as follows [3, 11]:

$$w(r, t) = -\frac{2}{\pi} \frac{1}{K} \int_r^a \frac{1}{\sqrt{(\xi^2 - r^2)}} \int_0^\xi \frac{m(\sigma + p_0 q) \, dm}{\sqrt{(\xi^2 - m^2)}} \, d\xi. \tag{10}$$

The method of successive approximations [11] can be used to solve for w in eqn (10). For the first approximation, the wave-effect integrals Q_1 and Q_2, i.e. $p_0 q$ are dropped temporarily and eqn (10) reduces to the associated static equation [3]. The reduced equation can be integrated to be the first approximation [3] as follows:

$$w_1(r, t) = w^0(r, t) = 2p_0(\sqrt{(a^2 - r^2)} - w_q^1/\alpha)/\pi K \tag{11}$$

where

$$\alpha = p_0/Y$$

and

$$w_q^1 = \begin{cases} \int_l^a (\xi^2 - l^2)^{1/2}(\xi^2 - r^2)^{-1/2}\,d\xi, & r < l \\ \int_r^a (\xi^2 - l^2)^{1/2}(\xi^2 - r^2)^{-1/2}\,d\xi, & l < r < a \end{cases} \tag{12}$$

The first approximation of the normal stress can be obtained by dropping Q_1 and Q_2 in eqn (4) and integrated in terms of eqn (11) for $r > a$ as follows[3]:

$$\sigma_{zz}^1 = \sigma_{zz}^0 = \frac{2p_0}{\pi}\left[\frac{aB}{\sqrt{(r^2 - a^2)}} - \sin^{-1}\frac{a}{r} + \frac{1}{\alpha}\int_l^a \frac{\xi\,d\xi}{\sqrt{[(r^2 - \xi^2)(\xi^2 - l^2)]}}\right] \tag{13}$$

where

$$B = 1 - (1 - l^2/a^2)^{1/2}/\alpha. \tag{14}$$

Equations (11) and (13) are the same as the corresponding equations for the associated static problem[3] and form a basis on which dynamic solutions are to be developed in the following sections. The finite stress condition at the crack tip is satisfied if B in eqn (13) is set equal to zero, this determined the plastic zone size for the associated static problem[3].

DYNAMIC CRACK SHAPE

The shape of the running Dugdale crack can be obtained from eqn (10) by including the integrals Q_1 and Q_2. To obtain closed-form solutions, it is assumed that the crack tip and the plastic zone tip are running at constant speeds of e and V, respectively; i.e. $l = et$ and $a = Vt$. The methods of successive approximation similar to those used in [9, 11] are to be used to obtain the crack shape function.

For convenience, an integral of $p_0 q$ in eqn (6), Q_1 in eqn (7) and Q_2 in eqn (8) are defined as follows:

$$I = \int_0^\xi (\xi^2 - m^2)^{-1/2} m p_0 q\,dm = \rho c_1 L I_1 + \mu L_2 I_2 \tag{15}$$

where

$$I_1 = \int_0^\xi (\xi^2 - m^2)^{-1/2} m Q_1\,dm, \quad I_2 = \int_0^\xi (\xi^2 - m^2)^{-1/2} m Q_2\,dm. \tag{16}$$

The first approximation of Q_2, i.e. Q_2^1 is obtained if eqn (11) is substituted into eqn (8). In substitution, the time derivative of the transform of eqn (11) is obtained as[3, 11]:

$$\frac{\partial \hat{w}_1^0}{\partial t} = \frac{2p_0}{\pi K}\left[\frac{\sin(sa)}{s} Ba\dot{a} + \frac{l\dot{l}}{\alpha}\int_l^a \frac{\sin(ns)\,dn}{s\sqrt{(n^2 - l^2)}}\right]. \tag{17}$$

In terms of eqn (17) and Q_2^1, the first approximation of I_2 in eqn (16) is obtained as follows:

$$I_2^1 = \int_0^\xi m(\xi^2 - m^2)^{-1/2} Q_2^1\,dm = BI_{21} + I_{22}^1 \tag{18}$$

where

$$I_{21} = -\frac{2p_0}{\pi K}\frac{\partial}{\partial \xi}\int_0^t G_2(\xi, t, a, \tau) a\dot{a}\,d\tau \tag{19}$$

$$I_{22}^1 = \frac{-2p_0}{\pi K \alpha}\frac{\partial}{\partial \xi}\int_1^{V/e} \frac{1}{\sqrt{(\lambda^2 - 1)}}\int_0^t G_2(\xi, t, \lambda l, \tau) l\dot{l}\,d\tau\,d\lambda \tag{20}$$

and

$$G_2(\xi, t, a, \tau) = \int_0^\infty \cos(\xi s)\cos[sc_2\eta(t - \tau)]\sin(as)s^{-1}\,ds. \tag{21}$$

In eqn (20), λ results from the transformation $n = \lambda l$ in eqn (17). I_{21} in eqn (19) is equal to $-I_2$ in [11] which was integrated into closed forms. In other words, the techniques used to integrate I_2 in [11] can readily be used to integrate eqn (21) into closed forms. Similar techniques can also be used to integrate eqn (20). After integrations, the results multiplied by μ can be written as [9, 11]:

$$\frac{\mu I_{21}^1}{p_0 v_2^2(1-\nu)} = \begin{cases} (\eta + v_2)^{-2}\xi, & \xi < a \\ 2\eta(a\eta - v_2\xi)(\eta^2 - v_2^2)^{-2}, & a < \xi < c_2\eta t \end{cases} \tag{22}$$

and

$$\frac{\mu I_{22}^1 \alpha}{p_0 D} = \begin{cases} D_{71}(\eta, e_2, 1)\xi, & \xi < l \\ [2\eta(\eta l - e_2\xi)D_{81}(\eta, e_2, \xi/l) + \xi D_{71}(\eta, e_2, \xi/l)], & l < \xi < a \end{cases} \tag{23}$$

where

$$v_2 = V/c_2, \quad e_2 = e/c_2 \quad \text{and} \quad D = (1-\nu)e_2^2. \tag{24}$$

The above quantities D_{71} and D_{81} are defined in the Appendix.

The integration techniques similar to those for Q_2^1 can be operated over eqn (7). The first approximation of eqn (7) is obtained as Q_1^1 in terms of eqn (17) and its integral similar to eqn (18) can be written as:

$$I_1^1 = \int_0^\xi m(\xi^2 - m^2)^{-1/2} Q_1^1 \, dm = BI_{11} + I_{12}^1 \tag{25}$$

where

$$I_{11} = \frac{2p_0}{\pi K}\frac{\partial}{\partial t}\int_0^t G_1(\xi, t, a, \tau) a\dot{a} \, d\tau \tag{26}$$

$$I_{12}^1 = \frac{2p_0}{\pi K\alpha}\frac{\partial}{\partial t}\int_1^{V/e} \frac{1}{\sqrt{(\lambda^2-1)}}\int_0^t G_1(\xi, t, \lambda l, \tau) l\dot{l} \, d\tau \, d\lambda \tag{27}$$

and

$$G_1(\xi, t, a, \tau) = \int_0^\infty \sin(\xi s)\sin[sc_1\eta(t-\tau)]\sin(as)s^{-1} \, ds. \tag{28}$$

The techniques for integrating eqn (21) can readily be applied to eqn (28) because they are very similar. In terms of eqn (28), I_{11} in eqn (26) and I_{12}^1 in eqn (27) can be integrated. The integrated form of $\rho c_1 I_{11}$ is equal to $k^2\eta\mu I_{21}$ if v_2 of I_{21} is replaced by v_1. Similarly, $\rho c_1 I_{12}^1$ is equal to $k^2\eta\mu I_{22}^1$ if e_2 of I_{22}^1 is replaced by e_1.

In terms of eqns (18) and (25) the first approximation of I in eqn (15) can be written as follows:

$$I^1 = \int_0^\xi (\xi^2 - m^2)^{-1/2} m p_0 q_1 \, dm = p_0 B q_0 \xi + \begin{cases} p_0 g_1/\alpha, & \xi \le l \\ p_0 h_1/\alpha, & l < \xi \le a \end{cases} \tag{29}$$

where

$$q_0 = (1-\nu)v_2^2[L_1(\eta + v_1)^{-2} + L_2(\eta + v_2)^{-2}]. \tag{30}$$

The operator L_1 results from L multiplied by η and is defined in the Appendix. The values of g_1 and h_1 above are equal to the values for $j = 1$ of the quantities as follows:

$$g_j = g_j^0\xi; \quad g_j = D^j(L_1 + L_2)D_{7j}(\eta, e_i, 1) \tag{31}$$

and

$$h_j = D^j(L_1 + L_2)l[2\eta(\eta - e_i\xi/l)D_{8j}(\eta, e_i, \xi/l) + D_{7j}(\eta, e_i, \xi/l)\xi/l]. \tag{32}$$

Where the subscript i is 1 for the operator L_1 and becomes 2 for the operator L_2. It can be seen that g_1 is equal to h_1 at $\xi = l$. At $\xi = a$, eqn (32) can be written as $h_1 = ah_1^0$, where h_1^0 is equal to the value of h_j^0 for $j = 1$ in the Appendix. If eqn (29) is substituted into eqn (10), the second approximation of the crack shape function is obtained as w_2 which has a form similar to its first approximation in eqn (11). The zeroth order Hankel transform of w_2 can be calculated as was done for w_1 and its time derivative can be written as:

$$\frac{\partial \hat{w}_2^0}{\partial t} = \frac{2p_0}{\pi K}\left\{\frac{\sin(sa)}{s}B_2\dot{a} + \frac{1}{\alpha}\int_l^a \left[\frac{l\dot{l}}{\sqrt{(\xi^2 - l^2)}} - \frac{\partial h_1}{\partial t}\right]\frac{\sin(s\xi)}{s}\,d\xi\right. \tag{33}$$

where

$$B_2 = B(1 - q_0) - h_1^0/\alpha. \tag{34}$$

The value of $\partial h_1/\partial t$ is equal to the value for $j = 1$ of the following equation:

$$\dot{h}_j = \partial h_j/\partial t = eD^jE_{j+1}(e_2, \xi/l) \tag{35}$$

E_2 above for $j = 1$ obtained from the time derivative of eqn (32) and is defined in the Appendix. If eqn (33) is substituted into eqn (8), the second approximation of Q_2, i.e. Q_2^2, is obtained. The second approximation of I_2 in eqn (16) is an integral over Q_2^2, which can be written in terms of eqns (19)–(21) and (33)–(35) as

$$I_2^2 = \int_0^\xi m(\xi^2 - m^2)^{-1/2}Q_2^2\,dm = B_2I_{21} + I_{22}^1 + I_{22}^2 \tag{36}$$

where the additional term, compared to (18), is

$$I_{22}^2 = \frac{2p_0}{\pi K\alpha}\frac{\partial}{\partial \xi}\int_1^{V/e} DE_2(e_2, \lambda)\int_0^t G_2(\xi, t, \lambda l, \tau)l\dot{l}\,d\tau\,d\lambda. \tag{37}$$

The integration of eqn (37) is similar to that for eqn (20) and the integrated results multiplied by μ are written as

$$\frac{\mu I_{22}^2\alpha}{p_0D^2} = \begin{cases} -D_{72}(\eta, e_2, 1)\xi, & \xi < l \\ -2\eta(\eta l - e_2\xi)D_{82}(\eta, e_2, \xi/l) + D_{72}(\eta, e_2, \xi/l)\xi, & l < \xi < a \end{cases} \tag{38}$$

where D_{72} and D_{82} are defined in the forms of D_{7j} and D_{8j} for $j = 2$ in the Appendix.

The second approximation of I_1 in eqn (16), i.e. I_1^2, is obtained using the integration procedures similar to those for I_2^2 and the results obtained are also similar to those for I_2^2 in eqns (37) and (38). In terms of I_1^2 and I_2^2, the second approximation of I in eqn (15), i.e. I^2, can be written as

$$I^2 = p_0B_2q_0\xi + \begin{cases} p_0(g_1 - g_2)/\alpha, & \xi \le l \\ p_0(h_1 - h_2)/\alpha, & l < \xi \le a \end{cases} \tag{39}$$

where g_2 and h_2 are obtained and defined as the special forms for $j = 2$ of the general expressions eqns (31) and (32) respectively.

All the higher order terms of g_j and h_j for j larger than 2 can be obtained from the procedures described above. At $\xi = a$, the value of h_j can be written as a h_j^0 where h_j^0 is defined in Appendix. The expression for the general jth order term $\dot{h}_j$ in eqn (35) can be obtained through differentiation of h_j with respect to time.

A clear pattern can be seen in the process of higher order approximations. After infinitely many approximations, the integral I in eqn (15) can be written in terms of eqns (31) and (32) as:

$$I = p_0 \bar{B} q_0 \xi - \begin{cases} p_0 \bar{g}\xi/\alpha, & \xi \le l \\ p_0 \bar{h} l/\alpha, & l < \xi \le a \end{cases} \tag{40}$$

where

$$\bar{g} = \sum_{j=1}^{\infty} (-1)^j g_j^0, \quad \bar{h}(\xi/l) = \sum_{j=1}^{\infty} (-1)^j h_j/l. \tag{41}$$

Furthermore, $\bar{B}$ in eqn (40) is found to be the product of two series, one of which can be written into a simple form as follows[9]:

$$\bar{B} = \frac{B - H/\alpha}{1 + q_0}; \quad H = \sum_{j=1}^{\infty} (-1)^{j-1} h_j^0. \tag{42}$$

The final form of w comparable to eqn (11) is obtained as follows:

$$w = w^0 - \frac{2p_0}{\pi K} [\bar{B} q_0 \sqrt{(a^2 - r^2)} - w_q/\alpha] \tag{43}$$

where

$$w_q = \begin{cases} \displaystyle\int_r^l \bar{g}\xi(\xi^2 - r^2)^{-1/2}\,\mathrm{d}\xi + \int_l^a \bar{h} l(\xi^2 - r^2)^{-1/2}\,\mathrm{d}\xi, & r < l \\ \displaystyle\int_r^a \bar{h} l(\xi^2 - r^2)^{-1/2}\,\mathrm{d}\xi, & l < r < a \end{cases} \tag{44}$$

It will be shown later that $\bar{B}$ must be vanishing in order to satisfy the finite stress condition at the tip of the extended crack. The calculation of w under the condition of vanishing $\bar{B}$ will be described in the next section.

PLASTIC ZONE SIZE OF MOVING CRACK

The size of the plastic zone surrounding the propagating crack can be determined by satisfying the condition that stress singularities vanish at the tip of the extended crack. In order to satisfy the finite stress condition, the normal stress σ_{zz} in eqn (4) must be calculated. The zeroth-order Hankel transform in eqn (5) can be obtained from eqn (43) as follows:

$$\frac{\pi K}{2p_0} \hat{w}^0 = (1 - \bar{B} q_0) \int_0^a \frac{\sin(s\xi)}{s} \xi\,\mathrm{d}\xi + \frac{1}{\alpha} \int_0^l \bar{g} \frac{\sin(s\xi)}{s} \xi\,\mathrm{d}\xi + \frac{1}{\alpha} \int_l^a (l\bar{h} - \sqrt{(\xi^2 - l^2)}) \frac{\sin(s\xi)}{s}\,\mathrm{d}\xi. \tag{45}$$

In terms of eqn (45), the first term on the right hand side of eqn (4) can be calculated. The second term on the right hand side of eqn (4) can be calculated from Abel's transforms in terms of eqns (15) and (40) as follows:

$$p_0 q = \frac{2}{\pi} \frac{1}{r} \frac{\mathrm{d}}{\mathrm{d}r} \int_0^r I\xi(r^2 - \xi^2)^{-1/2}\,\mathrm{d}\xi. \tag{46}$$

The integrations of eqn (4) in terms of eqns (5), (45) and (46) exactly recover the prescribed boundary conditions in eqn (1) on the extended crack surface for $r \le a$. To find the crack stresses, eqn (4) is further integrated using the techniques similar to those used in [9, 11]. After combinations and cancellations of terms involved in the integrations of eqns (5) and (46), the

normal stress in eqn (4) is obtained for $r > a$ as follows:

$$\sigma_{zz}\frac{\pi}{2p_0}=\frac{\bar{B}K_I a}{\sqrt{(r^2-a^2)}}+\frac{1}{\alpha}\int_l^a \frac{\xi}{\sqrt{(\xi^2-l^2)}\sqrt{(r^2-\xi^2)}}\,d\xi-\frac{\pi}{2}+\left(\frac{\pi}{2}-\sin^{-1}\frac{a}{r}\right)$$
$$\times\left[1+(1-\nu)v_2^2\bar{B}(L_1+L_2)2\eta v_i(\eta^2-v_i^2)^{-2}\right.$$
$$\left.-\frac{1}{\alpha}\sum_{j=1}^{\infty}(-1)^j D^j(L_1+L_2)2\eta e_i D_{8j}(\eta, e_i, V/e)\right] \tag{47}$$

where

$$K_I = 1+q_0-(1-\nu)v_2^2(L_1+L_2)2\eta(\eta-v_i)(\eta^2-v_i^2)^{-2}. \tag{48}$$

It is clear that the first term in eqn (47) is the only singular term. To satisfy the condition of finite stress at the extended crack tip, the first term in eqn (47) must be vanishing. This is achieved if either $\bar{B}$ or K_I is equal to zero. From calculations, it is determined that $\bar{B}$ vanishes at a lower crack speed than K_I does. Therefore, the vanishing of $\bar{B}$ in eqn (42) satisfies the finite stress condition and determines the size of the plastic zone.

The quantity $\bar{B}$ in eqn (42) consists of two main terms, B and the infinite series H of h_j^0 in the Appendix. The dynamic correction term h_j^0 is proportional to the jth power of D in eqn (24), which is in turn proportional to the square of the ratio between the crack speed and the shear wave speed, i.e. $e_2 = e/c_2$. Therefore, H can be seen as an alternating power series of e_2^2. If crack speed vanishes, i.e. $e_2 = 0$, H obviously becomes zero. Consequently, the finite stress condition $\bar{B} = 0$ reduces to the corresponding static condition of $B = 0$. For a propagating crack where e is not equal to zero, numerical calculations on H were carried out. The removable singular terms such as $(\lambda^2-1)^{-1/2}$ were removed by proper transformations such as $\lambda = \cosh u$. The terms h_1^0 and h_2^0 were calculated by means of the regular four point integration formula using an IBM 360/65 electronic computer. The first power term of H, h_1^0, is found numerically to be of the order of 10^{-1} and the second power term h_2^0 is 10^{-3}. Thus, H in eqn (42) converges very rapidly and it appears practically accurate enough to calculate only h_1^0, and h_2^0 for H. For various values of its non-dimensional parameters e_2 and l/a, the value of H at $\nu = 0.3$ was calculated and shown in Fig. 1. The value of B in eqn (14) was also calculated and shown in the

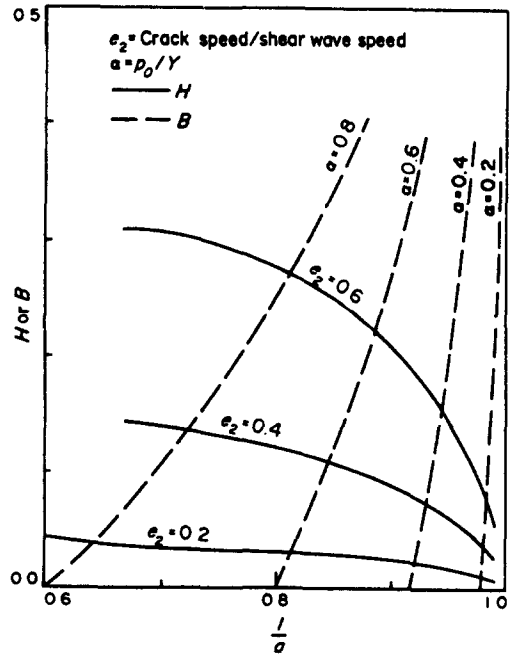

Fig. 1. Curves of nondimensionalized functions H and B for determining the plastic-zone size.

same figure. The intersection of the curve of B and the curve for H/α gives the value of l/a at which $\bar{B}$ vanishes. The value of l/a depends upon the nondimensional parameters e_2, α and ν. The width of the plastic zone is a $-l$, and the ratio of the width to the crack radius $(a-l)/l$ is determined on the basis of the determined value of l/a for various values of α and e_2 at $\nu = 0.3$ as shown in Fig. 2. For values of α and e_2, different from those in Fig. 2, the plastic zone size can also be determined by interpolating the values of H and B in Fig. 1 at a proper l/a which makes $\bar{B}$ in eqn (42) vanishing.

The value of the crack-shape function w in eqn (43) can now be calculated, using the determined value of l/a at which $\bar{B}$ vanishes. Typical values of w are obtained and shown in Fig. 3 for various values of α and e_2 at $\nu = 0.3$.

CRACK OPENING DISPLACEMENT AND ENERGY RELEASE RATE

The crack opening displacement (C.O.D.) is defined as the separation of the crack surfaces at the tip of the actual crack, i.e. at $x = l$. This quantity has often been used as a criterion in ductile fracture mechanics. Under the condition of $\bar{B} = 0$, the C.O.D. can be determined from eqn (43) and can be written as:

$$w_l = \frac{2p_0}{\pi K} l f_w(e_2, \alpha, \nu) \tag{49}$$

where

$$f_w = \sqrt{(V^2/e^2 - 1)} - (V/e - 1)/\alpha + 1/\alpha \int_1^{V/e} (\lambda^2 - 1)^{-1/2} \bar{h}(\lambda)\, d\lambda. \tag{50}$$

The nondimensional dynamic C.O.D. correction function f_w was calculated using a computer and the values are shown in Fig. 2.

In energy consideration, the presence of a crack lowers the potential energy of a medium by an amount which can be calculated for an elastic medium in equilibrium [10, 13]. It is assumed

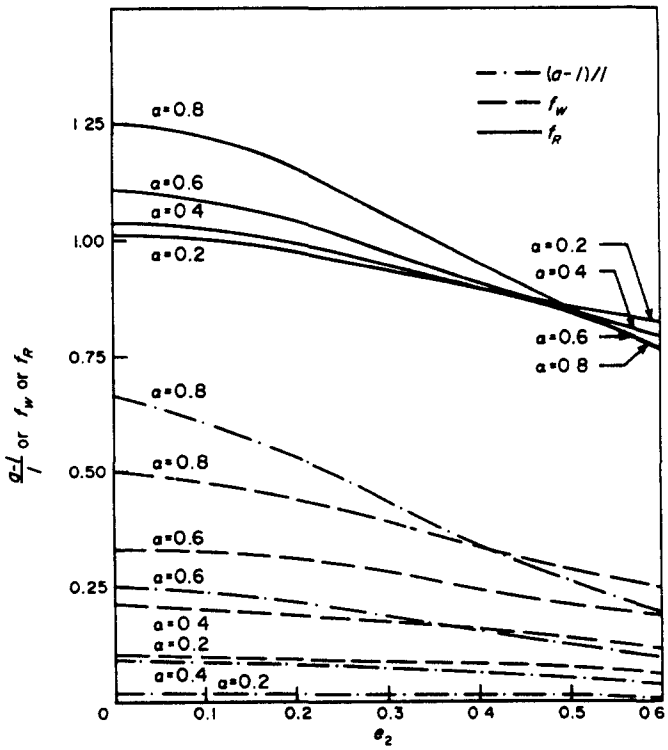

Fig. 2. Normalized plastic-zone width $(a-l)/l$ and the nondimensional dynamic correction curves of f_w for the C.O.D. and f_R for the energy release rate.

that the same method of calculation for the work done to the medium as was used in [10, 13] can also be used in the elastodynamic problem considered here. Therefore, the W_k work done to the medium by the crack surface pressure can be calculated from eqn (43). The derivative of W_k gives the total energy release rate which can be written as follows:

$$\frac{\partial W_k}{\partial l} = 2\frac{\partial}{\partial l}\left\{\int_0^l \pi r p_0 w \, dr - \int_l^a (Y - p_0)\pi r w \, dr\right\}$$
$$= 8(1-\nu^2)p_0^2 l^2 f_R(\alpha, V/e, e_2)/E \tag{51}$$

where

$$f_R = 1 + (V^3/e^3 - 1)(1+\alpha^{-2}) - 3(V/e - 1)/\alpha^2 - 2(V^2/e^2 - 1)^{3/2}/\alpha$$
$$+ \bar{g}/\alpha + 3/\alpha \int_1^{V/e} \bar{h}(\lambda)[\lambda - (\lambda^2 - 1)^{1/2}/\alpha] \, d\lambda. \tag{52}$$

The non-dimensional dynamic correction function for the total energy release rate f_R was calculated by the computer and also plotted in Fig. 2. $\partial W_k/\partial l$ in eqn (51) can be applied together with the rate of change of the surface energy to the extended Griffith theory [7, 10] to determine the condition under which a crack becomes unstable. Both the C.O.D. in eqn (49) and the energy release rate in eqn (51) can be seen as functions with an explicit factor of the crack radius l and reduce to the associated expressions when the dynamic effect terms $\bar{g}$ and $\bar{h}$ vanish.

DISCUSSION AND CONCLUSIONS

Dynamic effects in the propagation of a ductile penny-shaped crack in a perfectly plastic material were investigated using the methods of integral transforms [9, 11]. The crack is assumed to be the Dugdale crack with a constant yield stress at the crack tip under the action of a uniform tensile stress at infinity. An exact expression was obtained which satisfies the condition of the finite stress at the running crack tip, and the equation obtained was solved numerically to determine the size of the crack tip plastic zone. Exact expressions for the crack shape, the crack opening displacement, and the total energy release rate were also obtained. All those expressions were written as the product of explicit dimensional quantities and a dynamic correction function in terms of non-dimensional parameters. The dynamic correction functions were calculated using an electronic computer for various values of crack speeds and applied stresses. All the results obtained reduce to the associated static results when the crack speed tends to zero.

The width of the crack-tip plastic zone expressed in $(a-l)/l$ was determined and shown in Fig. 2. It can be seen that the width shrinks significantly with increasing crack speed. For different values of crack speed and applied stress than those shown in Fig. 2, the plastic zone

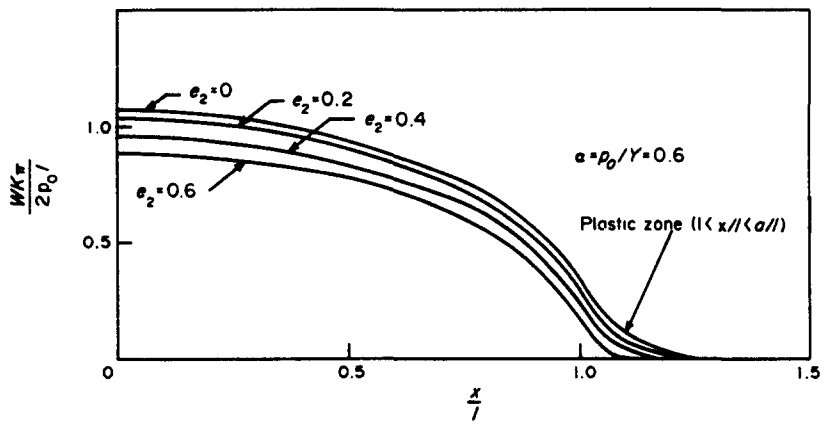

Fig. 3. Normalized crack shape $WK\pi/(2p_0 l)$ with its tip at $x/l = 1$ and plastic-zone tip at a/l.

size can be determined in terms of l/a by interpolating proper values of H and B in Fig. 1, which satisfy the finite stress condition $\bar{B} = 0$ in eqn (42).

The inertia effects of material particles resist the separation of the crack surfaces during propagation. Therefore, the entire crack size becomes smaller as crack speed increases as shown in Fig. 3. Similarly, the crack opening displacement and the total energy release rate were found to be decreasing with increasing crack speed as shown in Fig. 2. The curves in Figs. 1 and 2 are similar in shape but quite different in value in comparison with the corresponding two-dimensional results[9].

Acknowledgement—This research was supported by the Engineering Research Institute, Iowa State University, Ames, Iowa 50011.

REFERENCES

1. D. S. Dugdale, Yielding of steel sheets containing slits. *J. Mech. Phys. Solids* **8**, 100–104 (1960).
2. G. T. Hahn and A. R. Rosenfield, Local yielding and extension of a crack under plane stress. *Acta Met.* **13**, 293–306 (1965).
3. Y. M. Tsai, Stress distribution, crack shape and energy for a penny-shaped crack in a plate of finite thickness. *Engng Fract. Mech.* **4**, 155–169 (1972).
4. Z. Olesiak and M. Wnuk, Plastic energy dissipation due to a penny-shaped crack. *Int. J. Fract. Mech.* **4**, 383–395 (1968).
5. J. N. Goodier and F. A. Field, Plastic energy dissipation in crack propagation. *Fracture of Solids* (Edited by D. C. Drucker and J. J. Gilman), pp. 103–118. Interscience, New York (1963).
6. M. F. Kanninen, A. K. Mukherjee, A. R. Rosenfield and G. T. Hahn, The speed of ductile-crack propagation and the dynamics of flow in metals. *Mechanical Behavior of Materials under Dynamic Loads* (Edited by U. S. Lindholm), pp. 96–133. Springer-Verlag, New York (1968).
7. D. K. Felbeck and E. Orowan, Experiments on brittle fracture of steel plates. *Weld. Res. Suppl.* **34**, 570S–575S (1955).
8. R. G. Hoagland, A. R. Rosenfield and G. T. Hahn, Mechanisms of fast fracture and arrest in steels. *Met. Trans.* **3**, 123–136 (1972).
9. Y. M. Tsai, Dynamic ductile fracture of a central crack. *Proc. 13th Ann. Mtg. Soc. Engng Sci., JIAFS, NASA* (1976), pp. 247–256.
10. I. N. Sneddon, *Fourier Transforms*, pp. 430, 490. McGraw-Hill, New York (1951).
11. Y. M. Tsai, Exact stress distribution, crack shape and energy for a running penny-shaped crack in an infinite elastic solid. *Int. J. Fract.* **9**, 157–169 (1973).
12. G. N. Watson, *Theory of Bessel Functions*, 2nd Edn, p. 405. Cambridge University Press, Cambridge (1966).
13. Y. C. Fung, *Foundations of Solid Mechanics*, p. 5. Prentice-Hall, Englewood Cliffs, New Jersey (1965).

APPENDIX

$$Lg = \frac{2}{\pi}\int_1^\infty (\eta^2-1)^{-1/2} g(\eta)\,d\eta, \quad L_1 g = \frac{2}{\pi}\int_1^\infty \eta(\eta^2-1)^{-1/2} g(\eta)\,d\eta$$

$$L_2 g = \frac{8}{\pi}\int_1^\infty \eta^{-3}(\eta^2-1)^{1/2} g(\eta)\,d\eta + \frac{8}{\pi}\int_k^\infty \eta^{-3}(1-\eta^2)(\eta^2/k^2-1)^{-1/2} g(\eta)\,d\eta$$

$$D_{71}(\eta, e_2, \xi/l) = \int_{\xi/l}^{V/c} (\lambda^2-1)^{-1/2}(\eta+\lambda e_2)^{-2}\,d\lambda$$

$$D_{81}(\eta, e_2, \xi/l) = \int_1^{\xi/l} (\lambda^2-1)^{-1/2}\lambda(\eta^2-\lambda^2 e_2^2)^{-2}\,d\lambda$$

$$h_i^0 = D^i(L_1+L_2)2\eta(\eta c/V - e_i)D_{8i}(\eta, e_i, V/c)$$

$$\bar{E}_2 = [(\eta+\xi/c_2 t)^{-2} - 2\eta(\eta - e_2\xi/l)(\eta^2-\xi^2/c_2^2 t^2)^{-2}](\xi^2/l^2-1)^{-1/2}\xi^2/l^2 + 2\eta^2 D_{81}(\eta, e_2, \xi/l)$$

$$E_2(e_2, \xi/l) = (L_1+L_2)\bar{E}_2(\eta, e_i, \xi/c_i t, \xi/l)$$

$$D_{7i}(\eta, e_2, \xi/l) = \int_{\xi/l}^{V/c} E_i(e_2, \lambda)(\eta+\lambda e_2)^{-2}\,d\lambda$$

$$D_{8i}(\eta, e_2, \xi/l) = \int_1^{\xi/l} E_i(e_2, \lambda)\lambda(\eta^2-\lambda^2 e_2^2)^{-2}\,d\lambda.$$